CTE and other sensor effects in thick, fully depleted CCDs

Andrei Nomerotski
Brookhaven National Laboratory

SDW2017, Baltimore
28 September 2017

LSST Camera

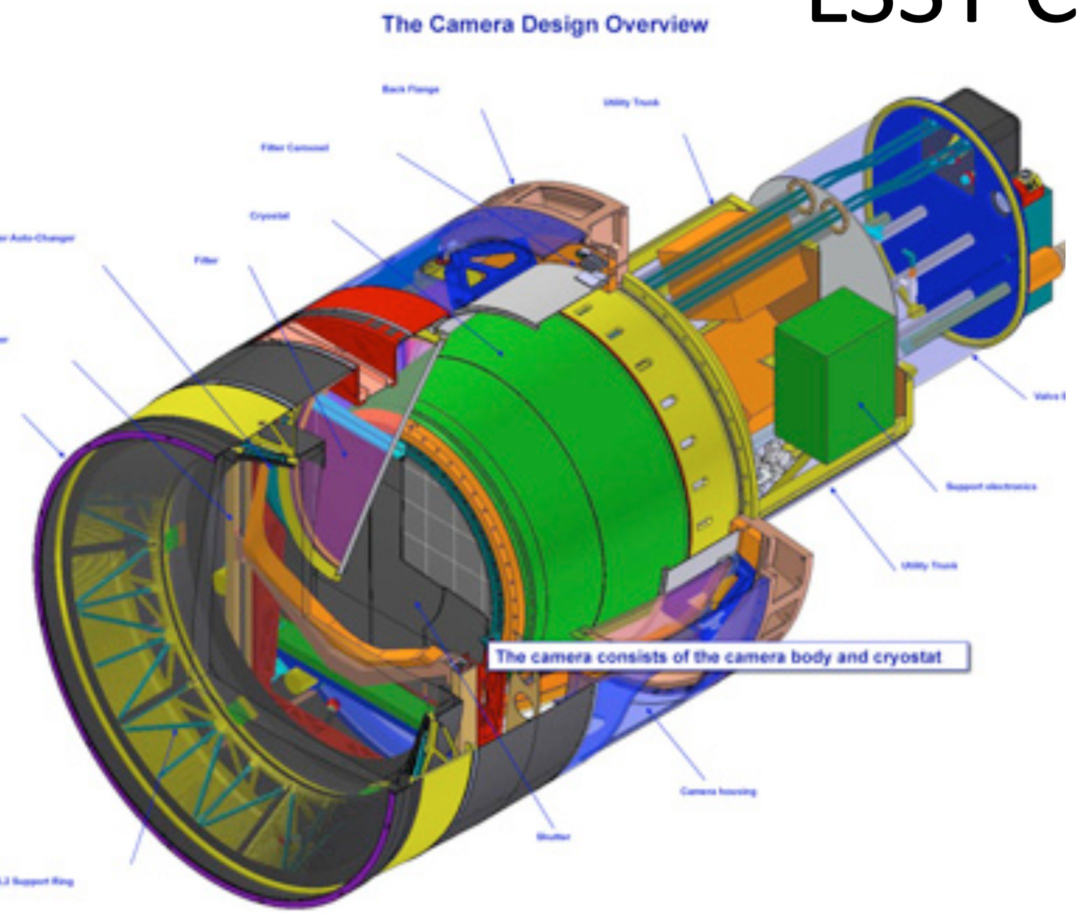

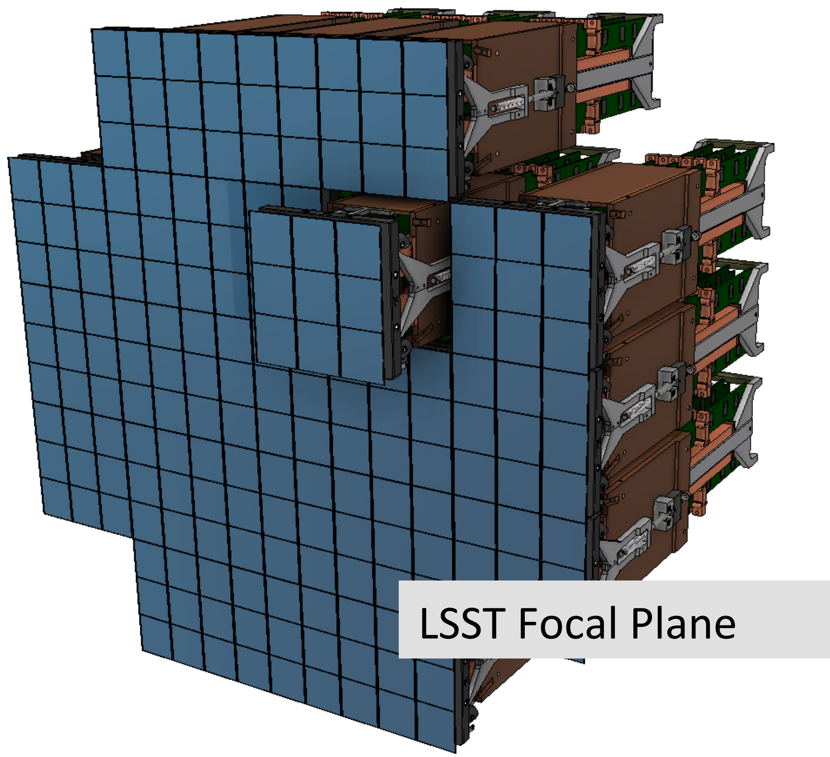

- 64cm diameter → 3.5°
- 189 CCDs → 3.1 Gigapixels
- 21 “rafts” with integrated electronics for nine CCDs

Raft Tower Module

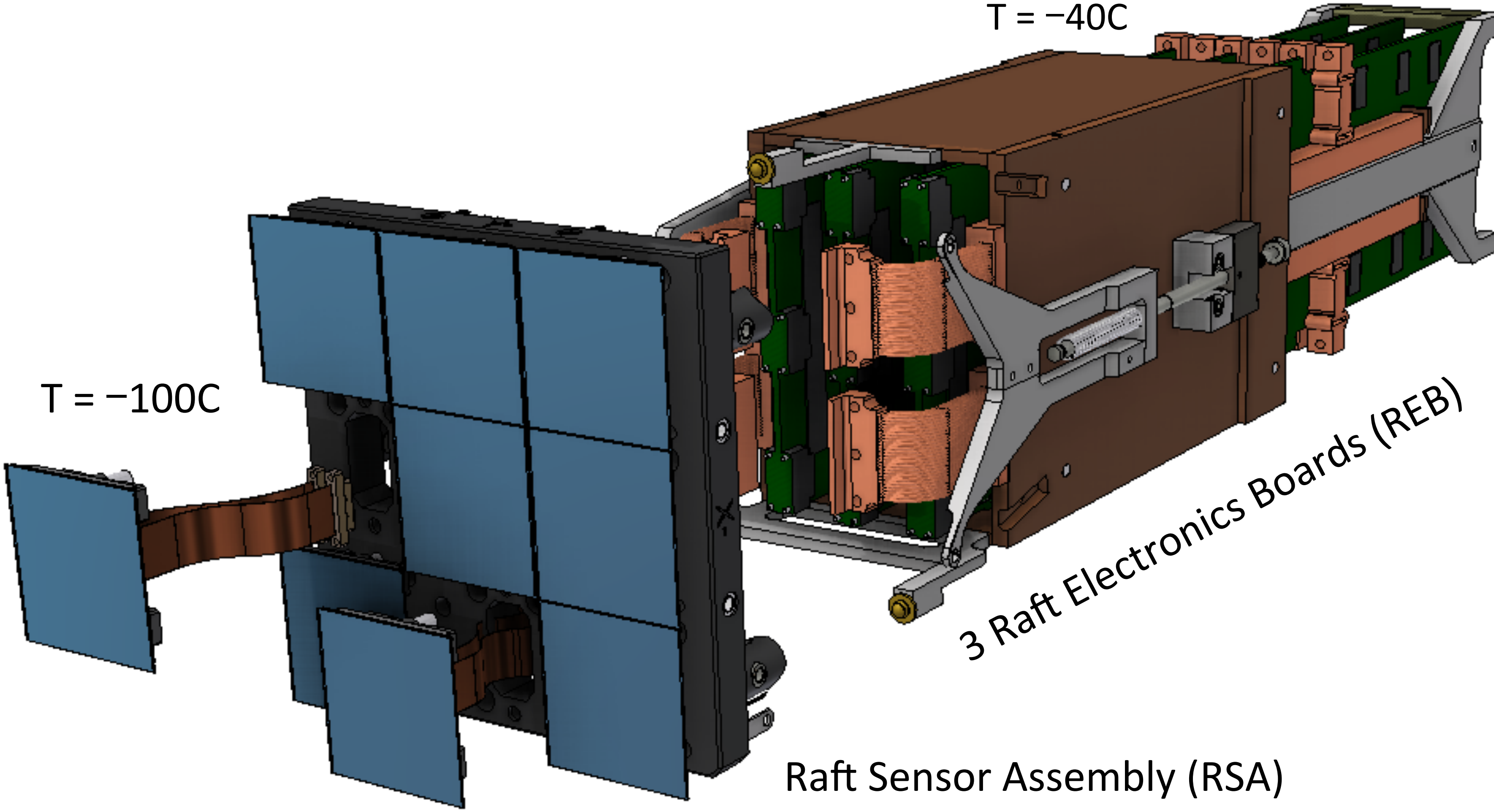

See Paul O’Connor’s talk

LSST CCD Sensor

- 4k x 4k = 16 Mpixels
- 10x10 microns pixel
- Noise spec 8 e-, based on anticipated sky noise; limits pixel rate
- Pixel read rate is 550 Kpix/s
- 2 second readout time spec → 16 amplifiers
- Si thickness 100 micron →
  Enhanced infrared response

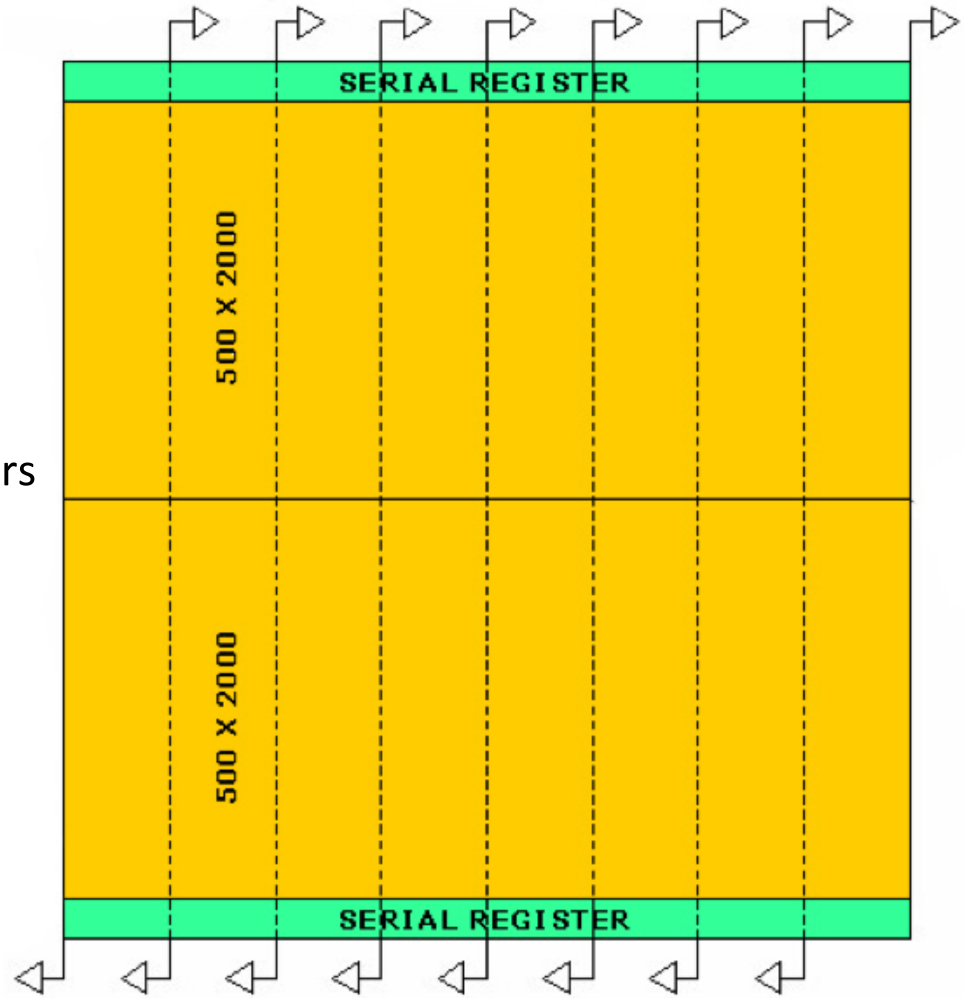

LSST CCDs

CCD250

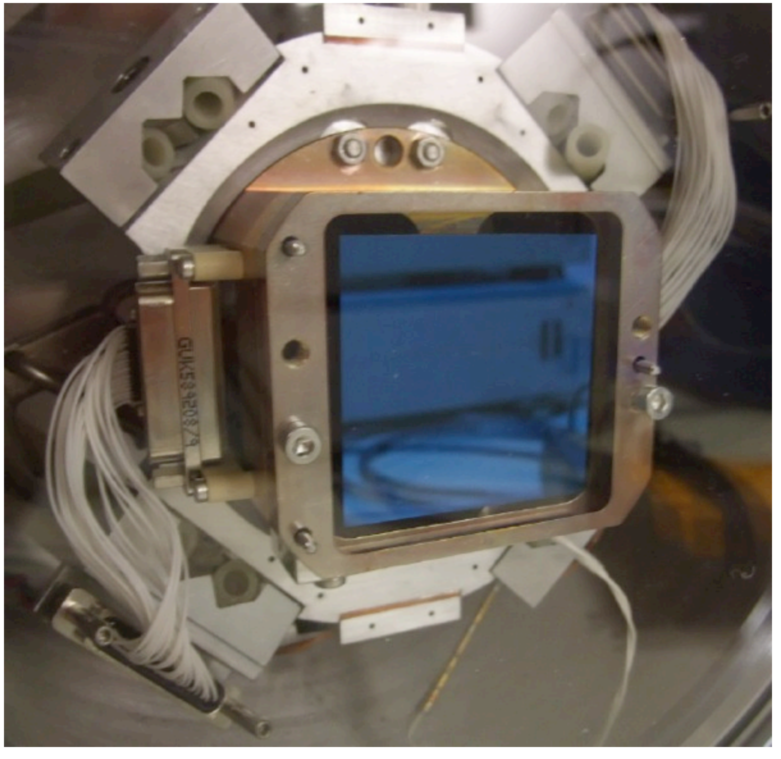

STA3800

On to more subtle things

LSST pixel : 10 x 10 x 100 micron^3
→ Pixels are skyscrapers

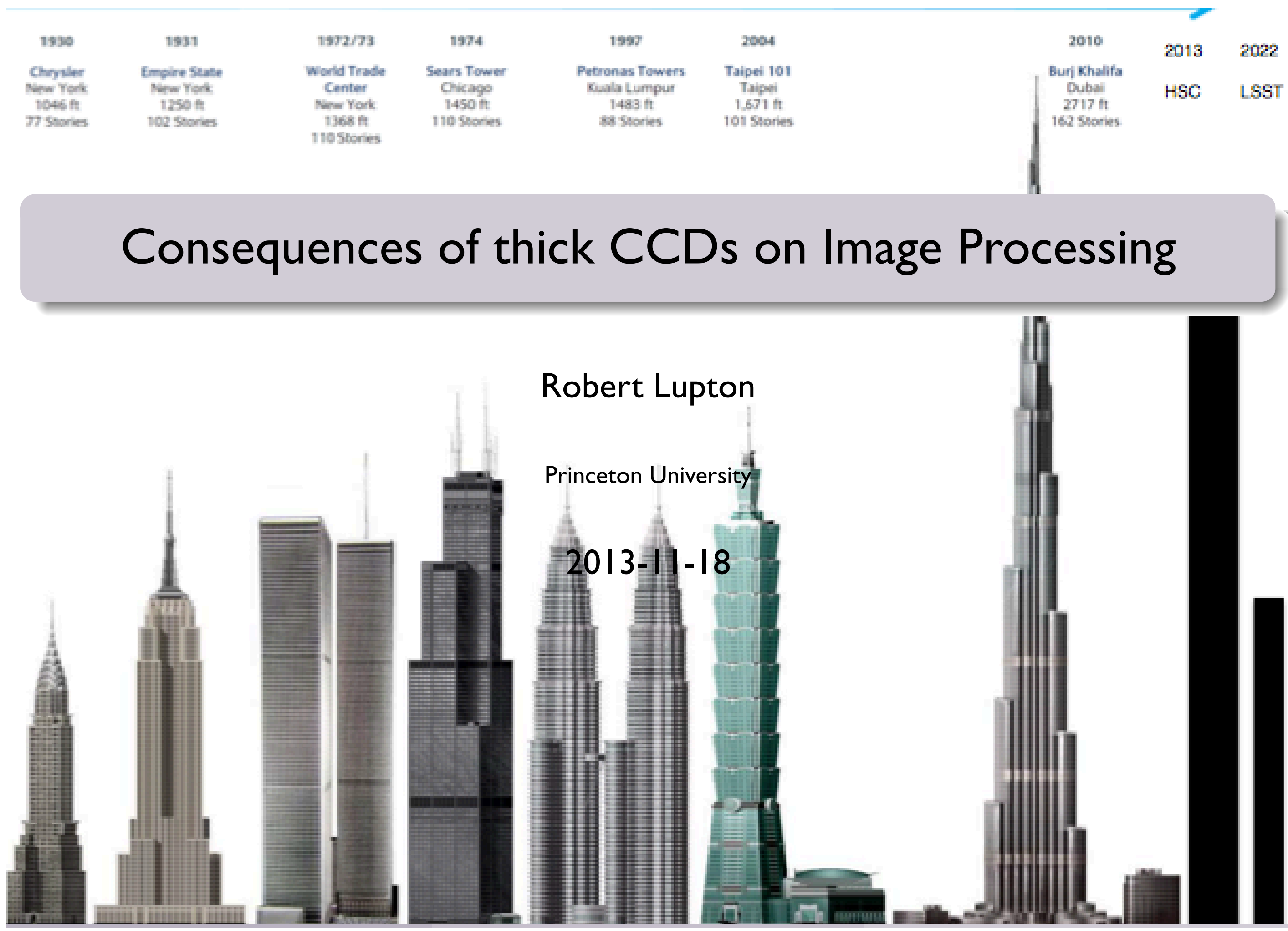

Consequences of thick CCDs on Image Processing

Robert Lupton

Princeton University

2013-11-18

What's the problem with thick CCDs?

Fully depleted CCD have a non-trivial electrostatics which lead to astrometric biases and PSF distortions

- Difficult to disentangle from photometric effects

Static : edge effects, tree-rings

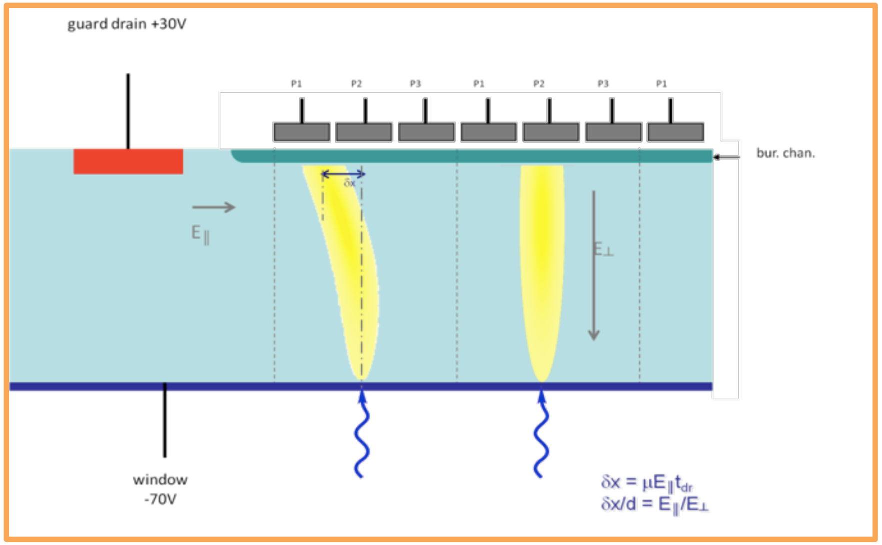

"Dynamic" : brighter-fatter effect

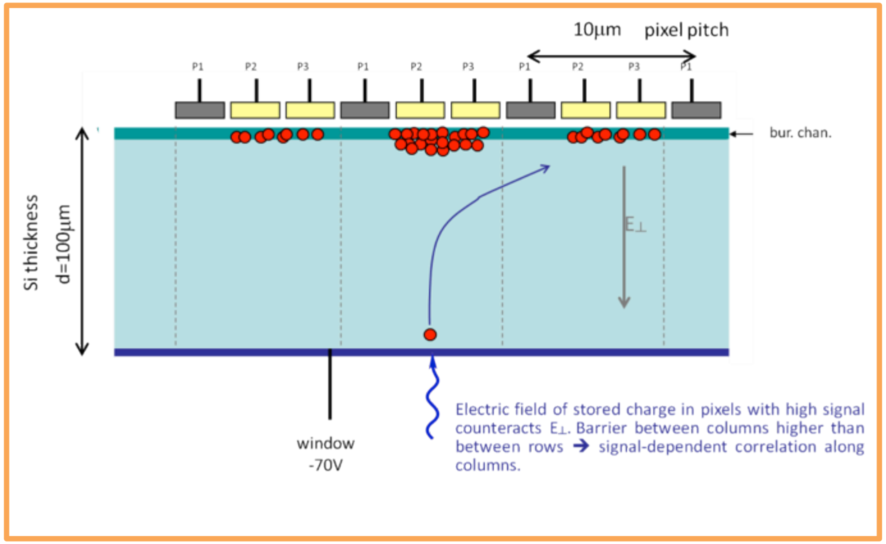

LSST Dark Energy Science Collaboration – DESC

Sensor Anomalies Working Group

- Main focus on CCD signatures, important for precision astrometry, photometry and shear measurement in LSST, WL is one of strongest motivations

Workshops “Precision Astronomy in Fully Depleted CCDs” at BNL

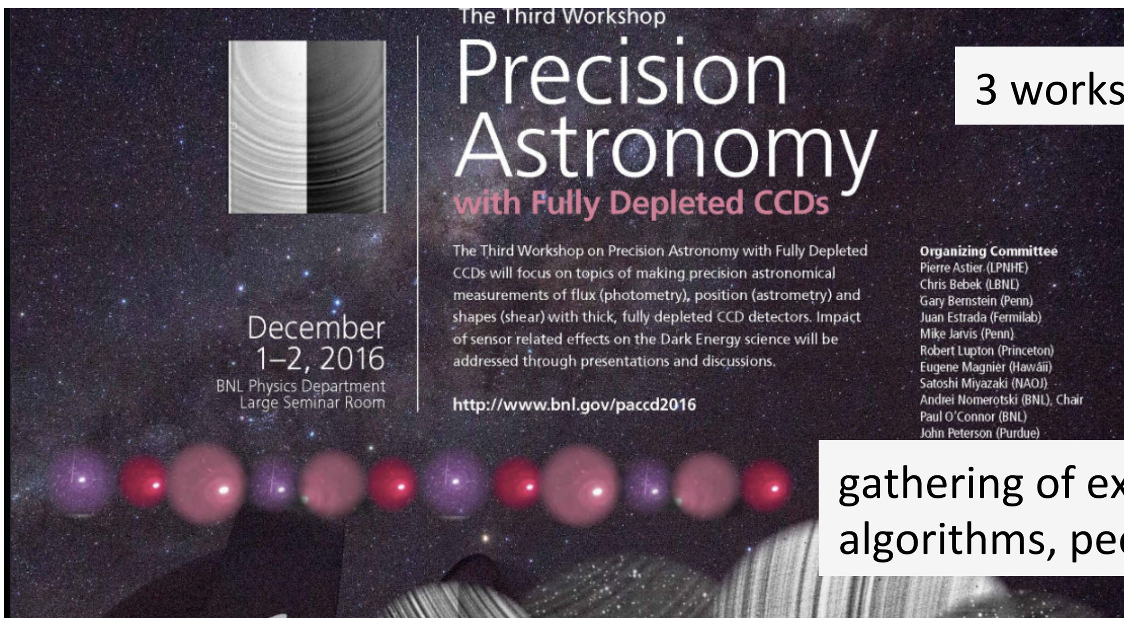

3 workshops: in 2013, 2014 and 2016

gathering of experts in CCDs and reduction algorithms, peer-reviewed proceedings in JINST

http://iopscience.iop.org/journal/1748-0221/page/extraproc60

Astrometric Distortions in Thick CCDs

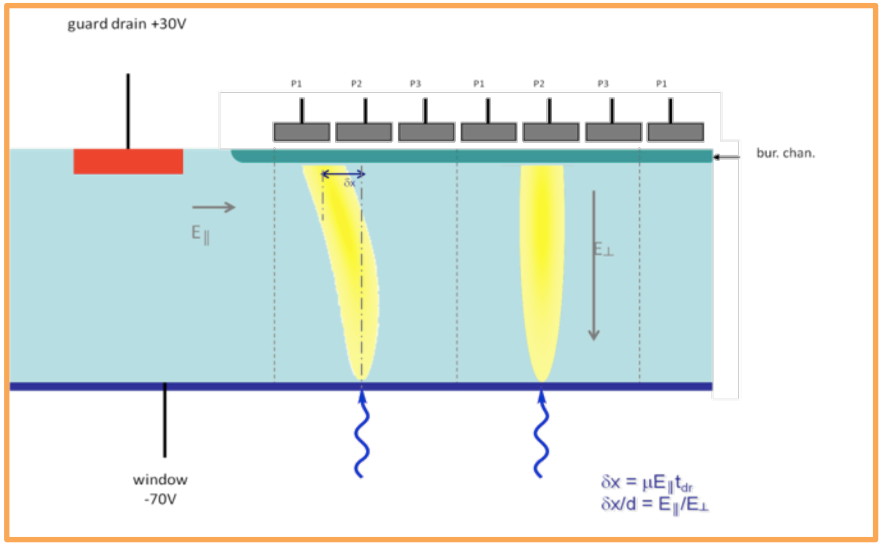

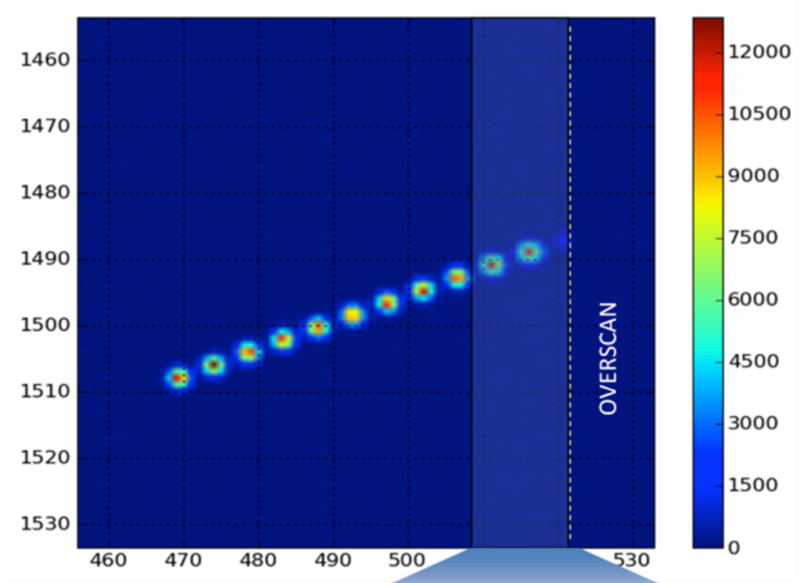

P O'Connor 2014 *JINST* **9** C03033

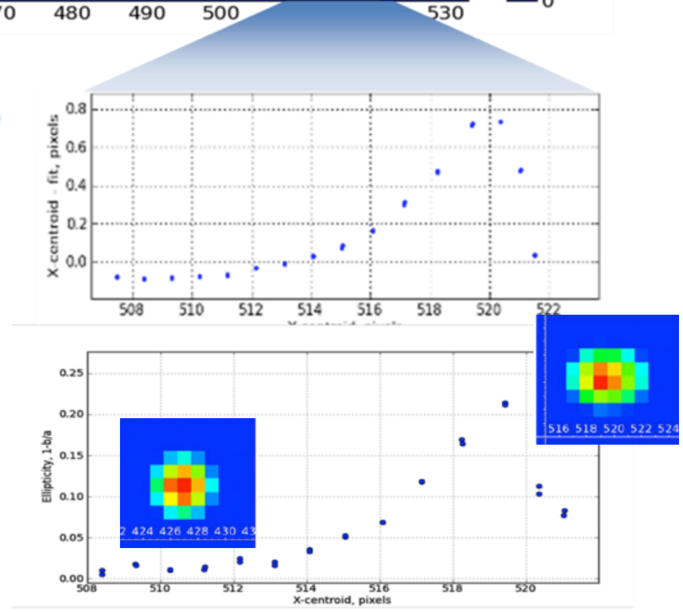

Distortions on the edge:

- Astrometric bias: up to 50%
- Ellipticity: up to 20%

Tree Rings in ITL sensors

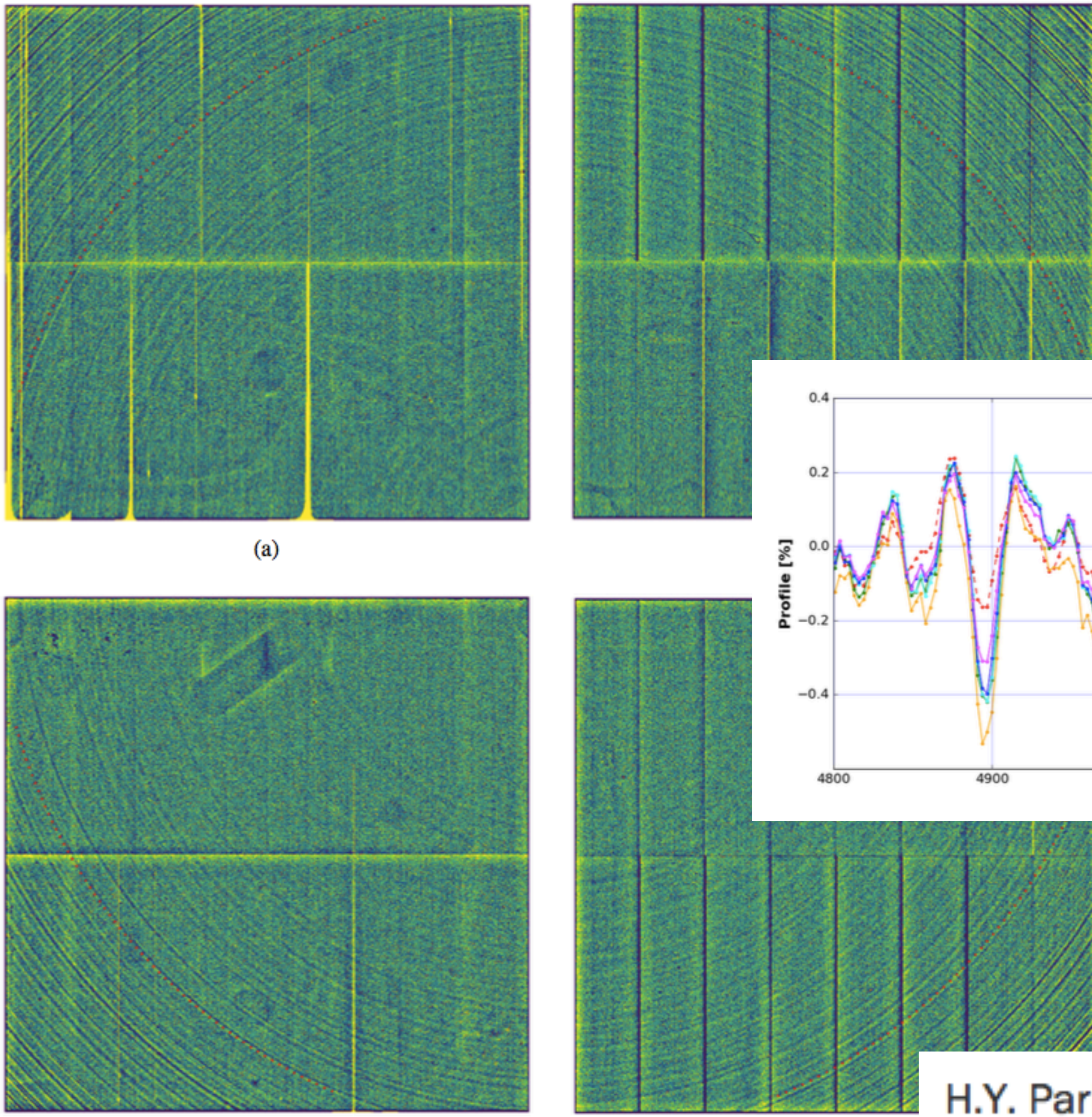

(a)

(c)

(d)

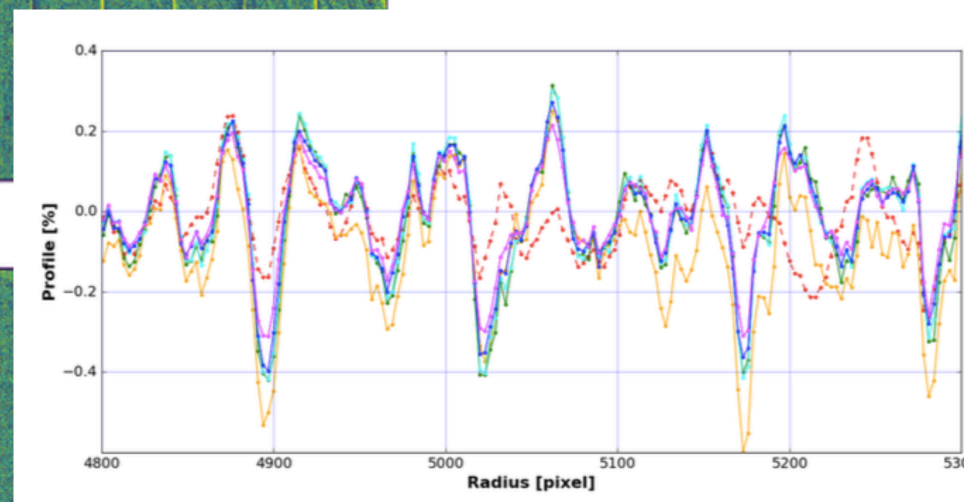

H.Y. Park *et al* 2017 *JINST* **12** C05015

Major effort to study BF effect

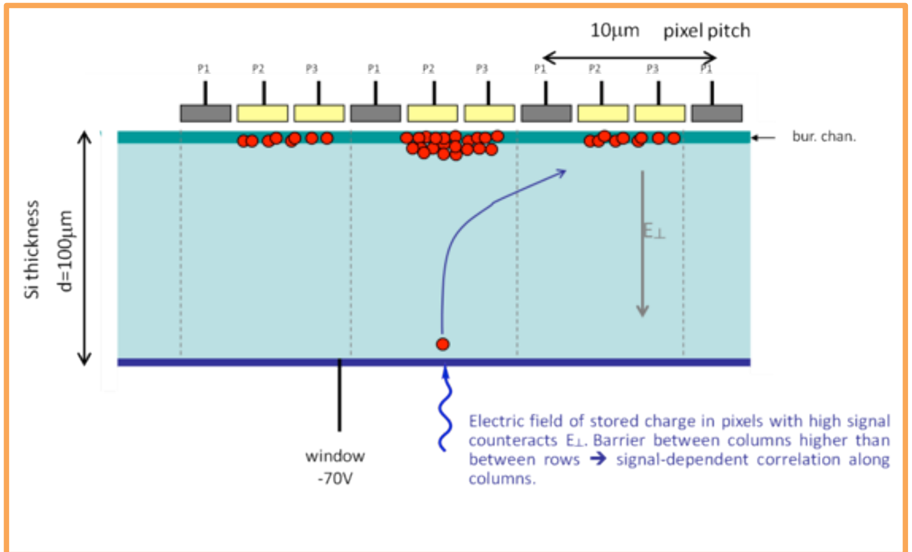

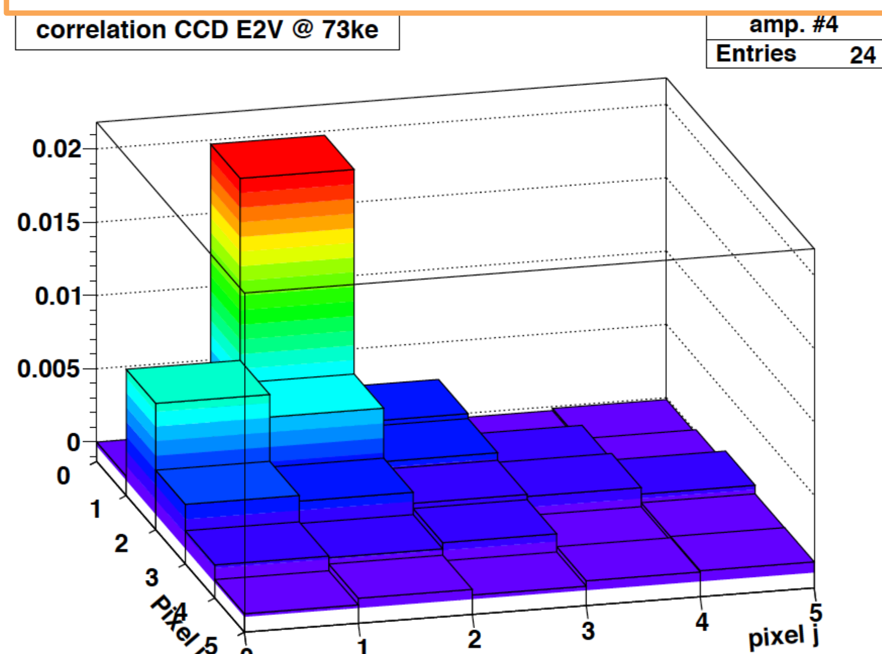

Pixel correlations

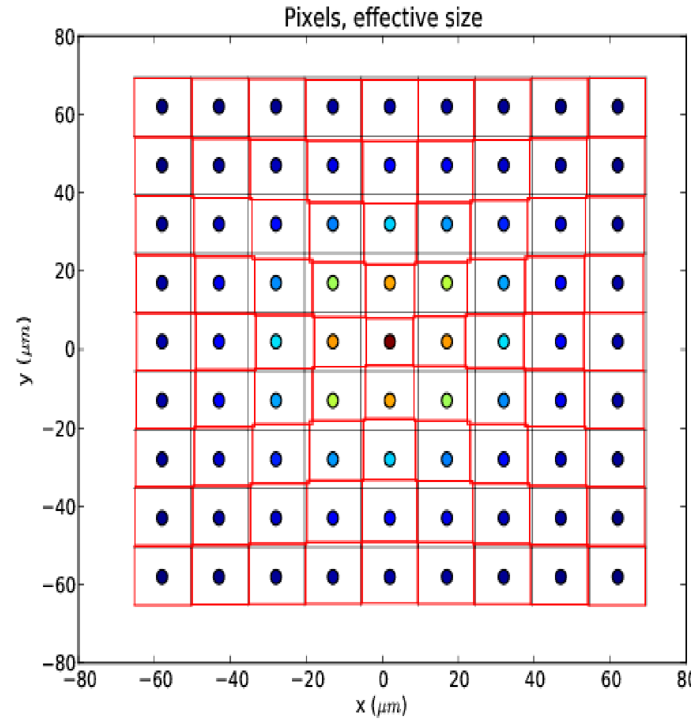

Correlations can be readily measured in flats and used to derive parameters of BF model for PSF

P Antilogus *et al* 2014 *JINST* **9** C03048

Poisson solver

Developed to model Brighter Fatter effect (Craig Lage, UC Davis)

C. Lage *et al* 2017 *JINST* **12** C03091

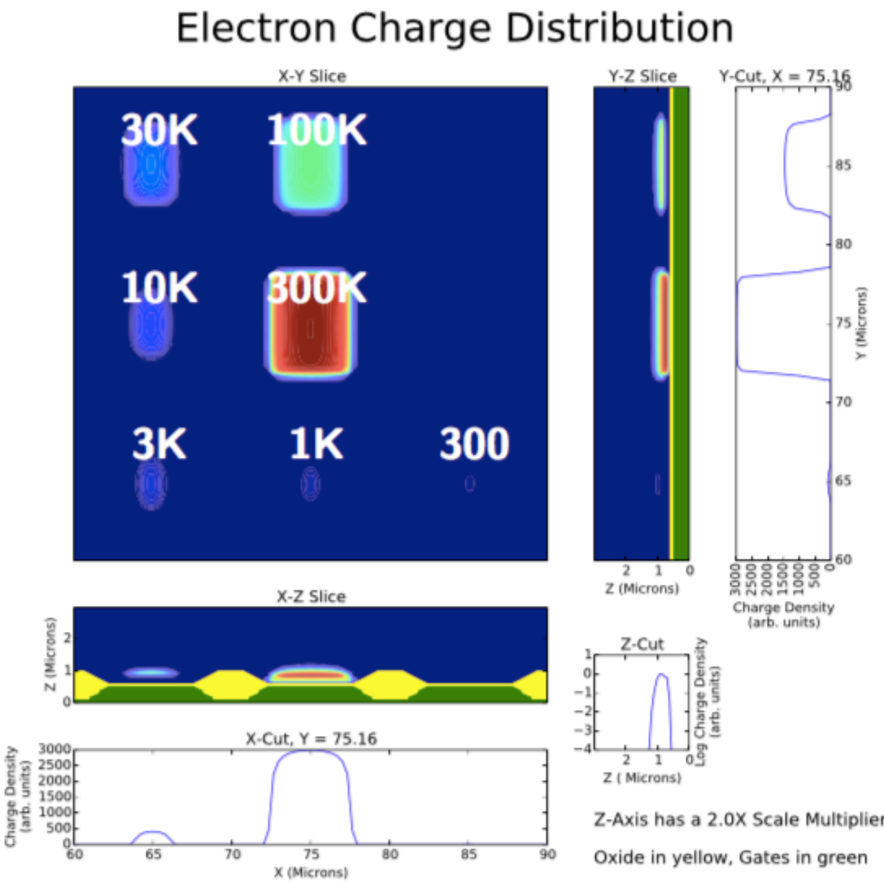

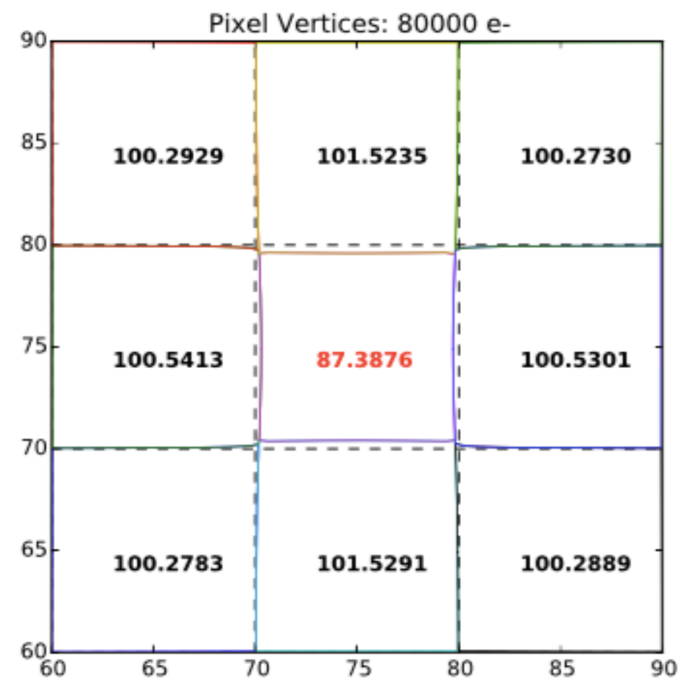

Success: same parameters describe PSF and correlations

Direct B-F - Measured:

$$X = 0.77 \pm 0.06; Y = 0.91 \pm 0.08$$

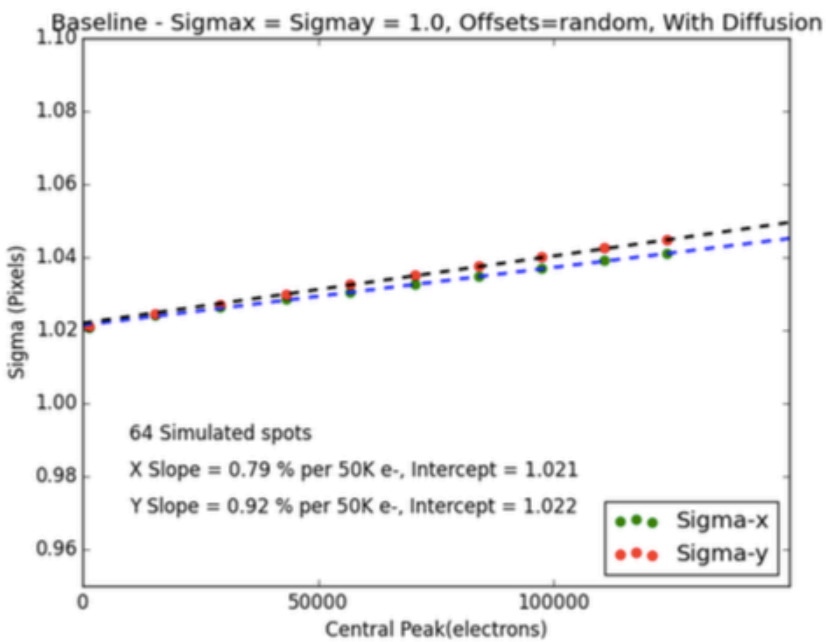

Pixel Correlations

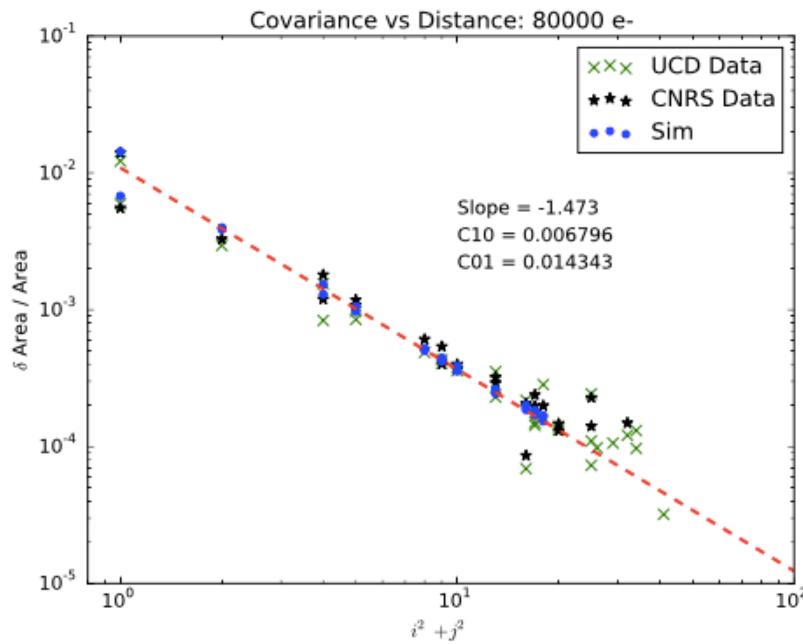

LSST Optical Simulator and Typical Spot Images

UC Davis 1:1 Re-Imager

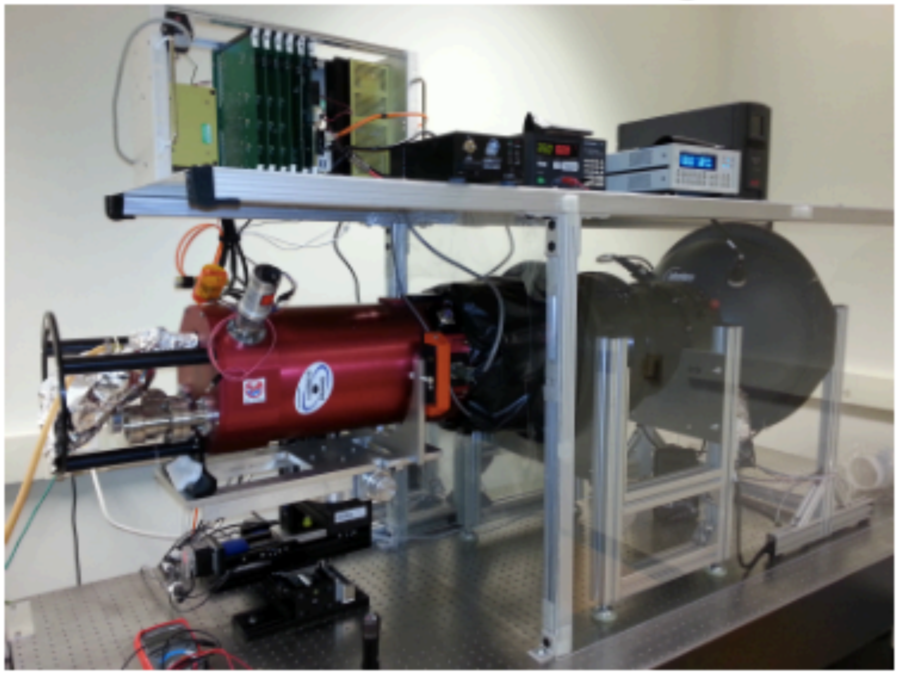

A. Bradshaw *et al* 2015 *JINST* **10** C04034

Typical Image of 30 micron Spots:

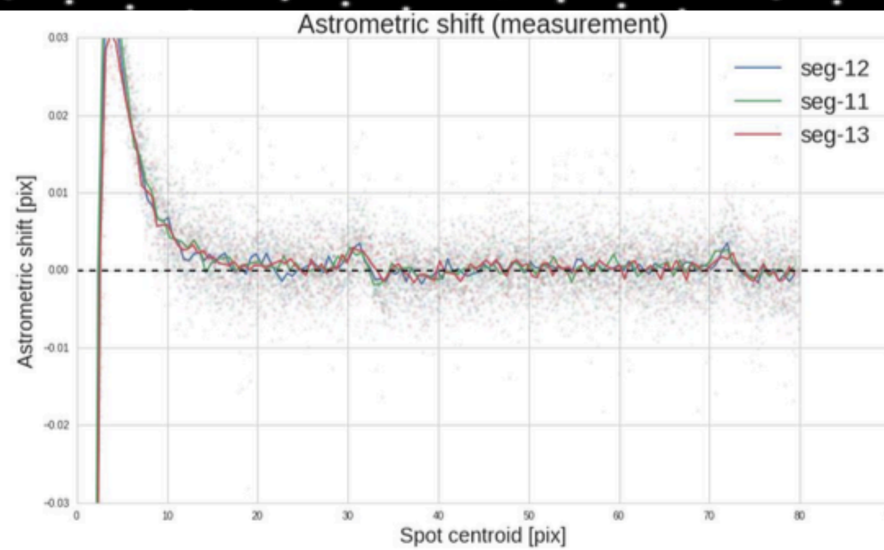

Tyson, et.al., "The LSST Beam Simulator", SPIE 9154-67 (2014), arXiv:1411.5667.

Fringe projector at BNL

- Michelson interferometer to generate sinusoidal variation of intensity
- Used to study Brighter Fatter effect

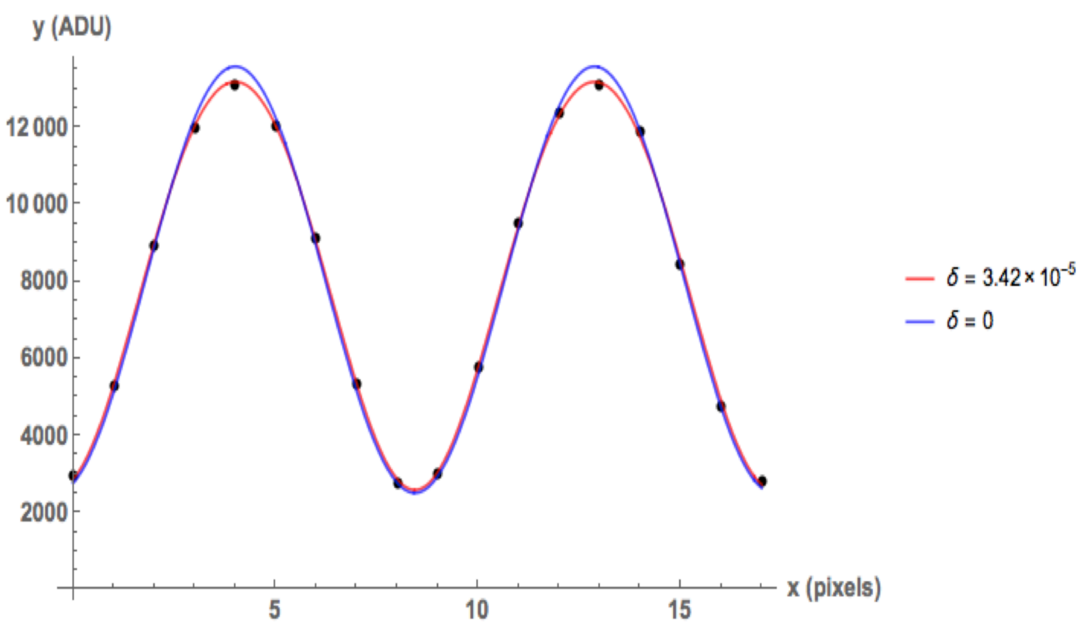

BF effect in fringes: data vs model

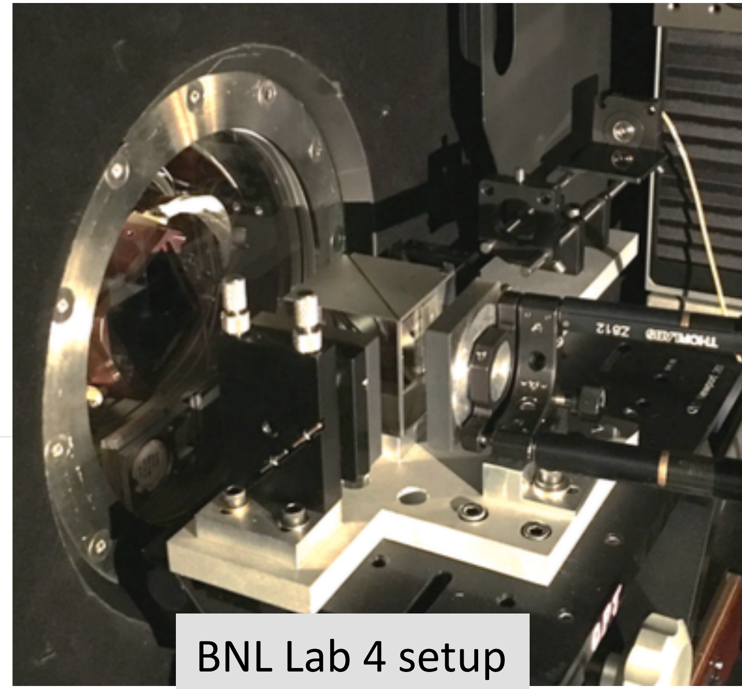

BNL Lab 4 setup

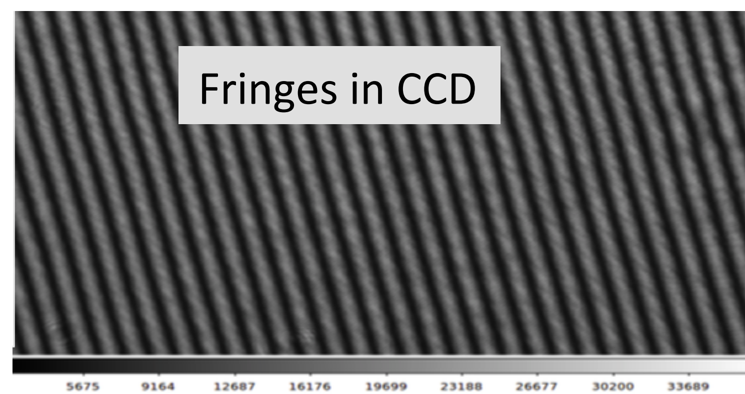

Fringes in CCD

W. Gilbertson *et al* 2017 *JINST* **12** C09009

More CCD characterization

Used cosmics to measure gain and diffusion in LSST CCDs

Cosmic ray in LSST CCD

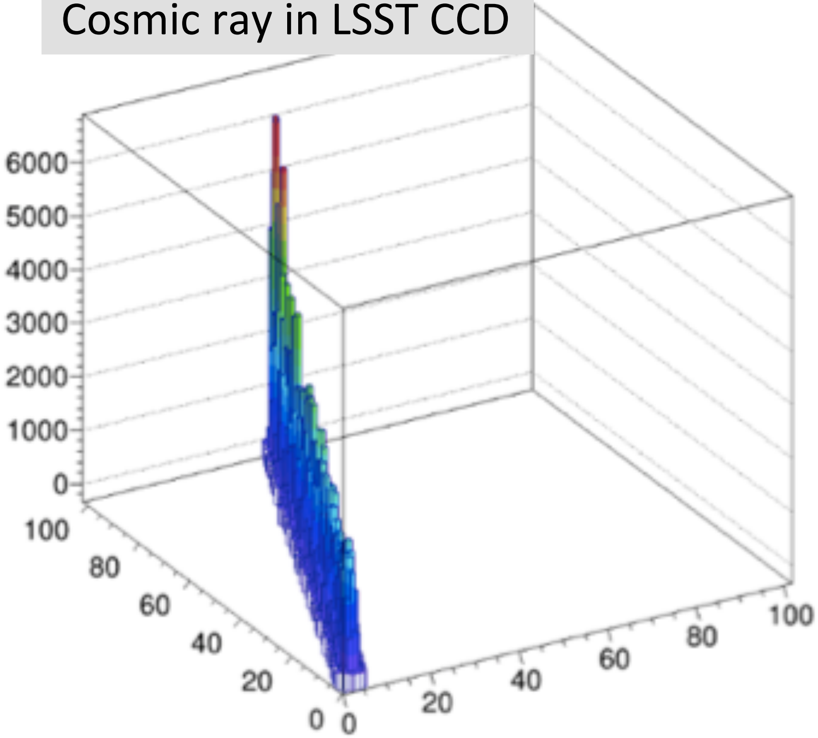

dE/dx in CCD

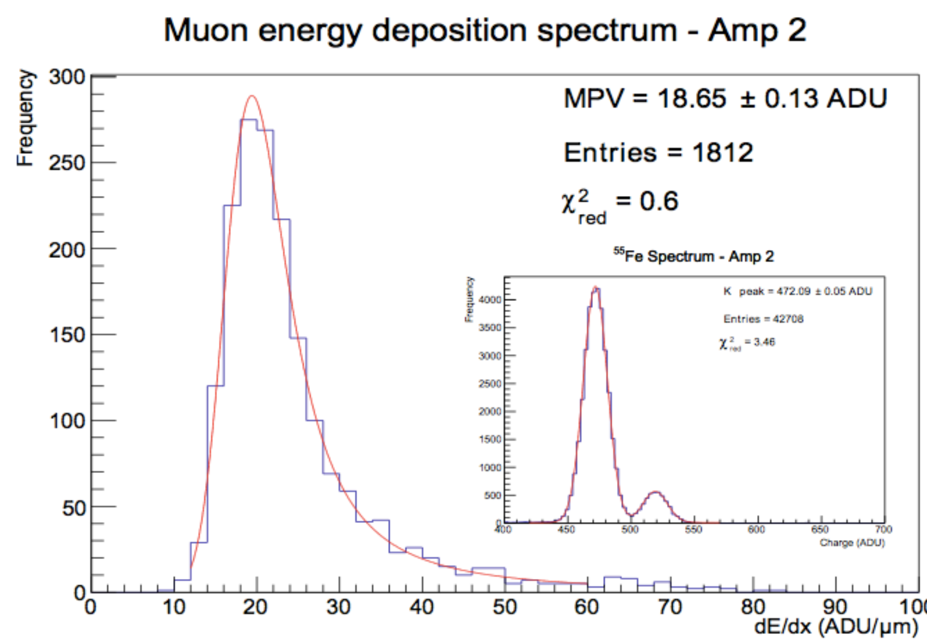

M. Fisher-Levine and A. Nomerotski 2015 *JINST* **10** C08006

CTE with Fe55

Using X-ray flats for CCD characterization

- Fe55 X-rays produce compact clouds of ~1600 electrons, < 1 um
- Standard gain calibration technique for CCDs, used also for diffusion measurements

- Hit shape is symmetric but lateral electric fields in CCD can distort it (edges, tree rings etc)

- Uniform irradiation, not sensitive to the surface
  30 micron conversion depth
  → can extract astrometry and decouple it from photometry

Easy to have good statistics, it's not too difficult to probe every pixel

→X-ray flat fielding, dataset of 7M hits

CTE in Fe55 x-rays

5.9 and 6.5 keV lines

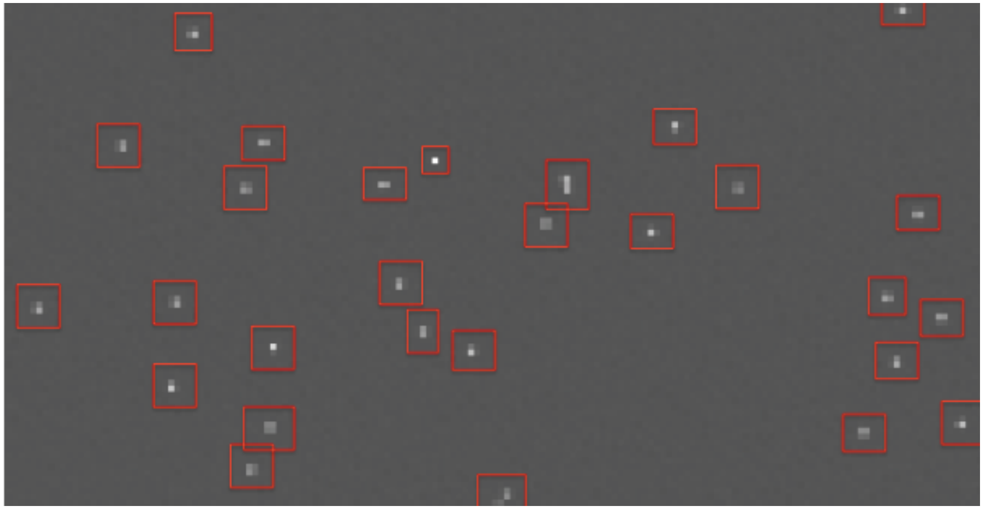

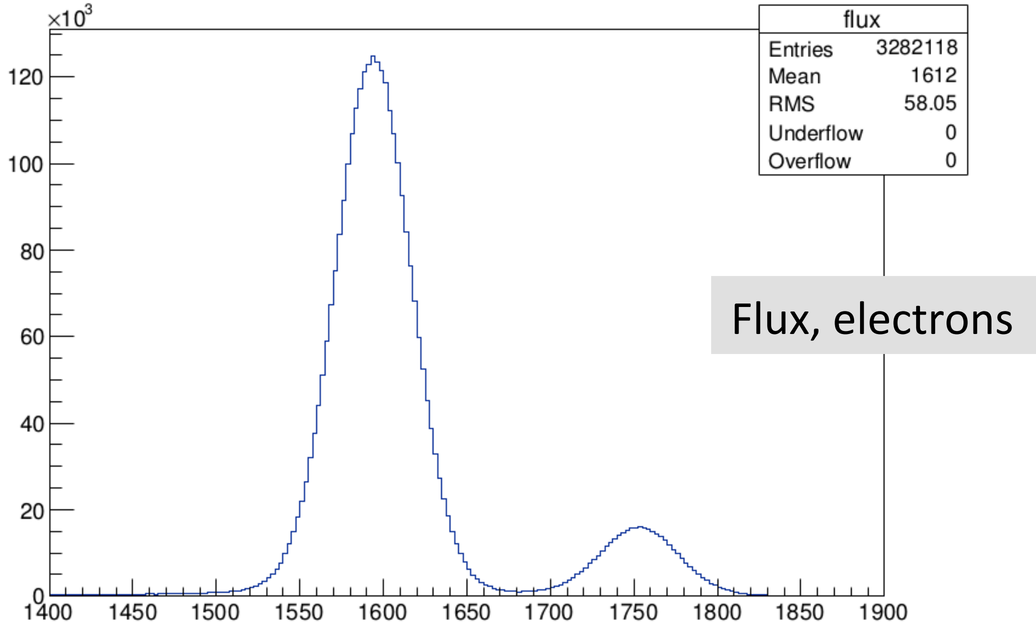

Diffusion in CCD

3.6 micron in 100 micron thick sensor

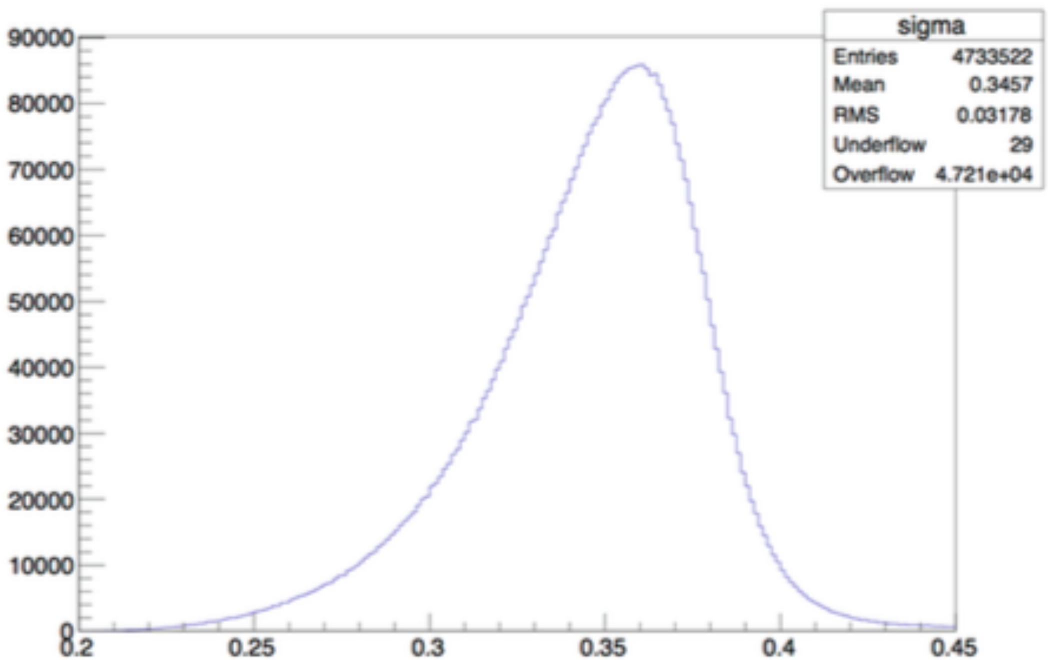

Figure 4 Distribution of the PSF size (sigma, in pixels) in the

Central pixel collects:

75 % for central hit
40% for side hit
25% for corner hit

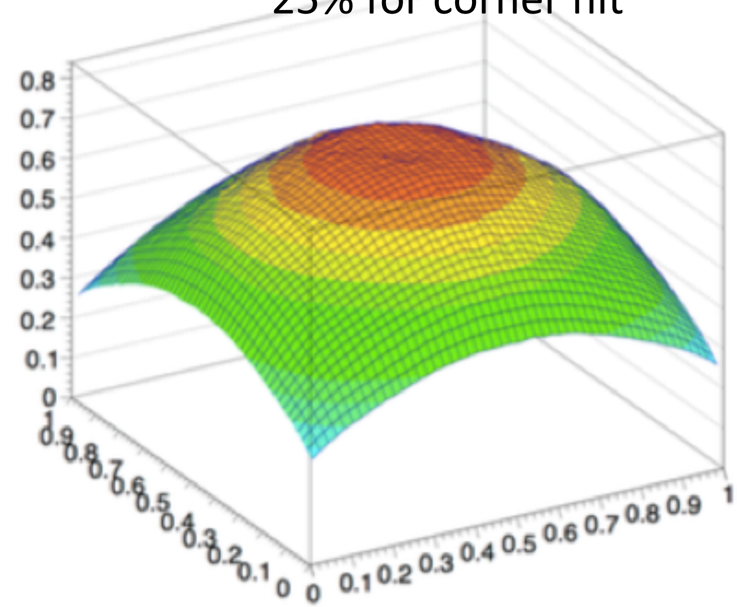

5.3 CTE Measurement Techniques

5.3.1 X-ray Transfer

X-ray transfer, as discussed in Chapter 2, is the standard method in measuring absolute CTE performance.[6] The technique is extremely valuable and is indispensable compared to other CTE measurement methods used which often give erroneous results. Figure 5.20 defines absolute CTE with the equation

$$\mathrm{CTE}_X = 1 - \frac{S_D(e^-)}{X(e^-)N_P}, \tag{5.19}$$

where CTE_X is the CTE as measured by x rays, $X(e^-)$ is the x-ray signal (e.g., 1620 e^- for an Fe^{55} x-ray source) and $S_D(e^-)$ is the average deferred charge after N_P pixel transfers (e^-).

Figure 5.21(a) shows a horizontal Fe^{55} x-ray transfer plot taken from a 520 × 520 CCD that exhibits a global CTE problem. The x-ray events interacting furthest from the on-chip amplifier experience the greatest charge loss. Note that the single-pixel-event line tilts "upward," whereas the deferred charge level for the first trailing pixel following the target pixel is seen as "downward" pattern

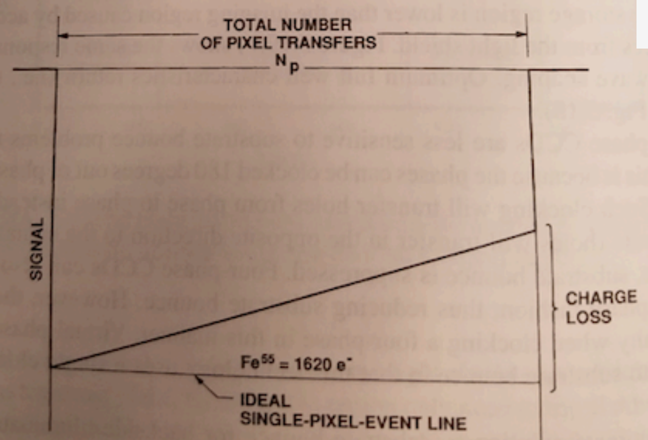

Figure 5.20 Absolute CTE definition using x-ray stimulation.

Janesick

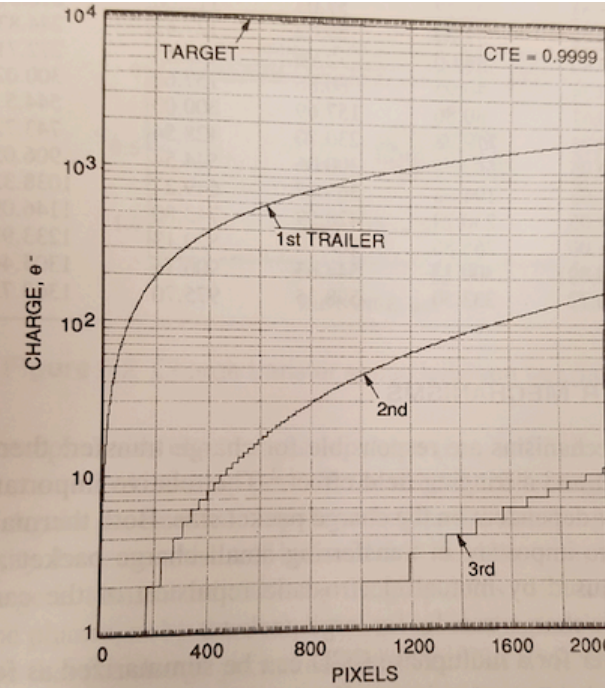

Figure 5.1(b) Theoretical 10,000-e^- point-source response assuming CTE = 0.9999.

Problem: need to integrate several pixels to collect all charge → Start collecting deferred charge → Textbook formula is not applicable

CTE observables

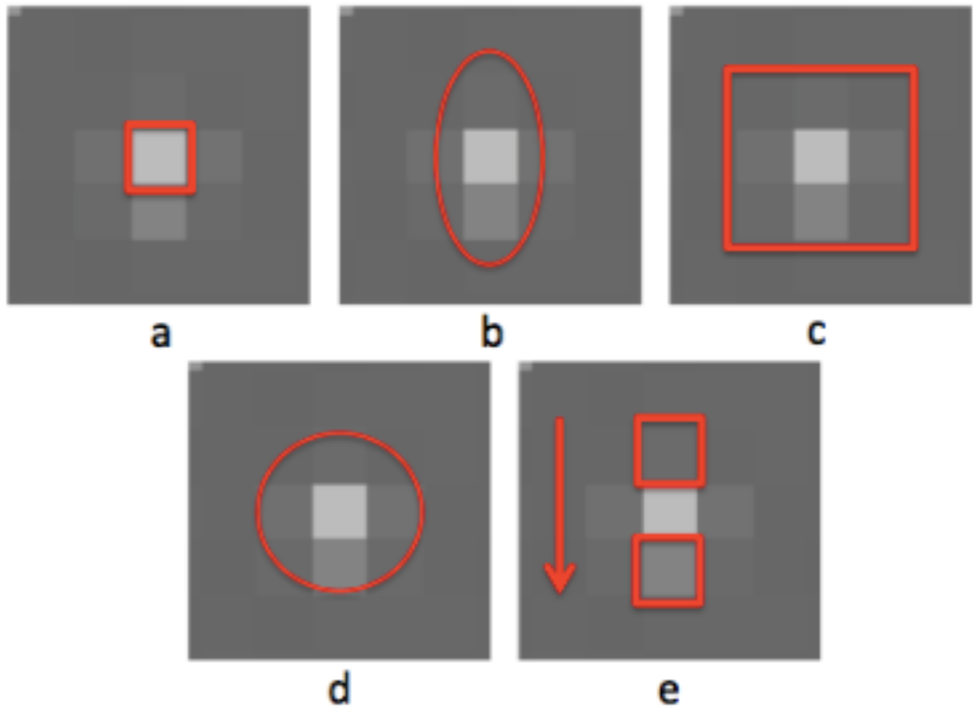

- MC simulations of Fe55 hits: assumes diffusion and random hit position
- Models deferred charge due to CTE

- Used this MC to predict behavior of observables as function of CTI

Differential Flux in MC

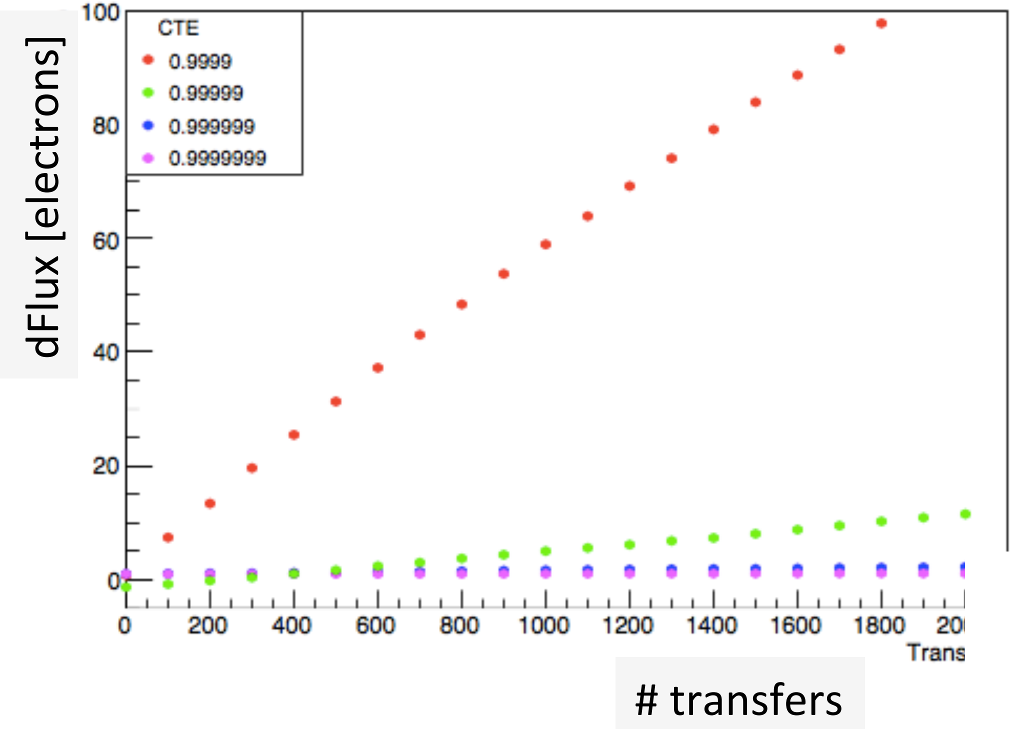

- Fit slopes for different CTI
- Plot slope [e/transfer] vs CTI

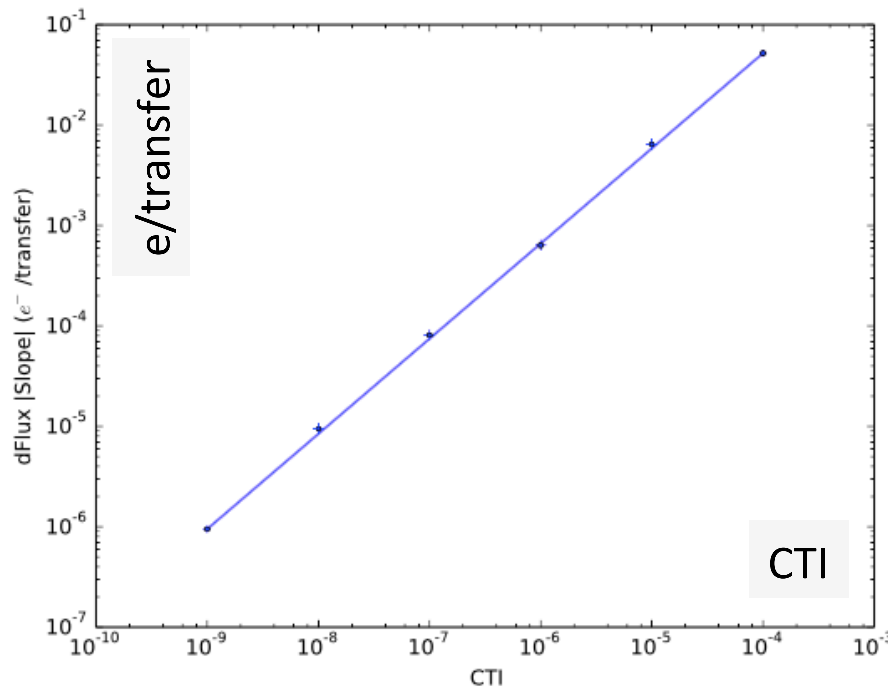

Slope vs CTI for all observables

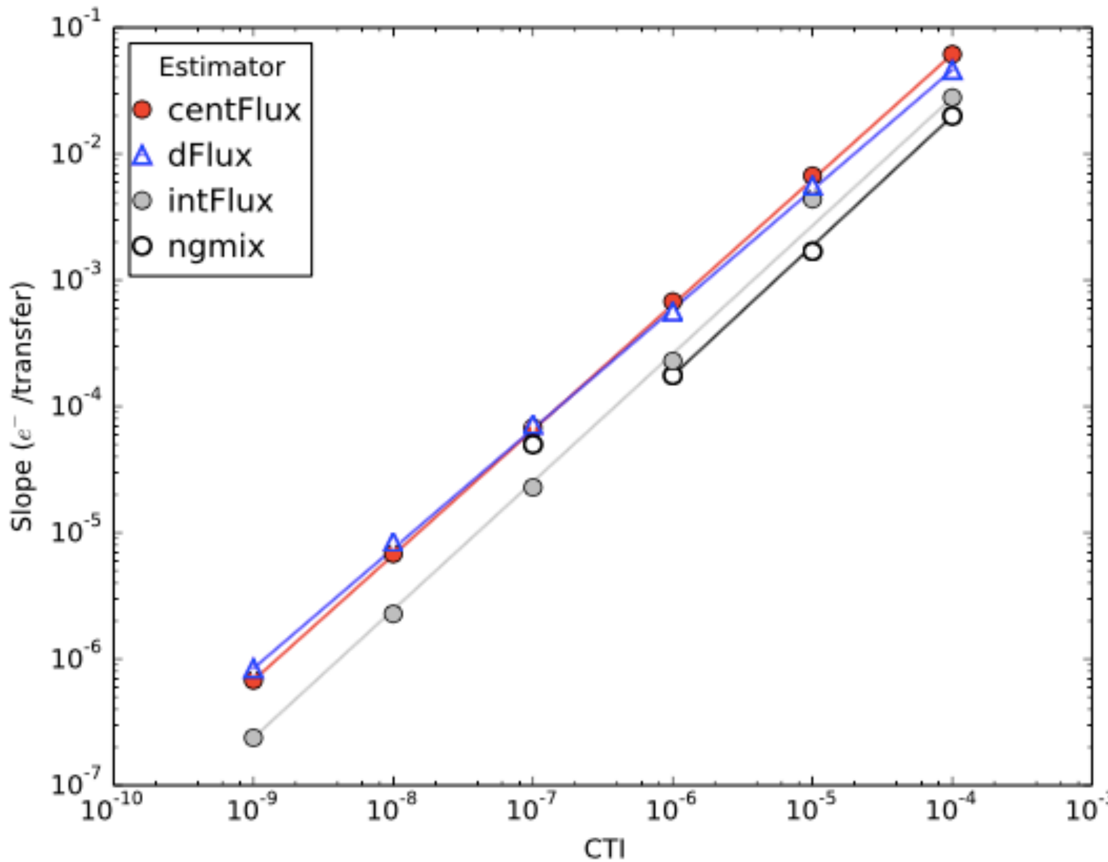

Differential variables are slightly more sensitive

D. Yates *et al* 2017 *JINST* **12** C07025

Example of parallel CTI in data

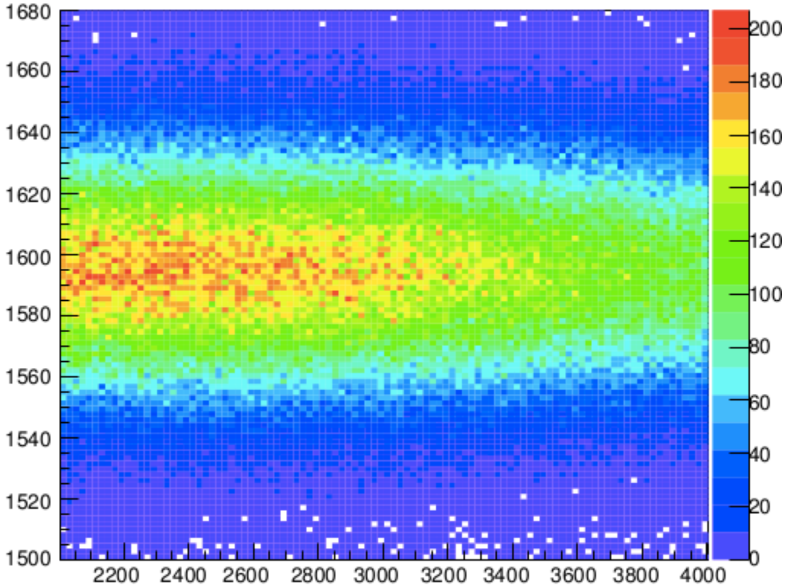

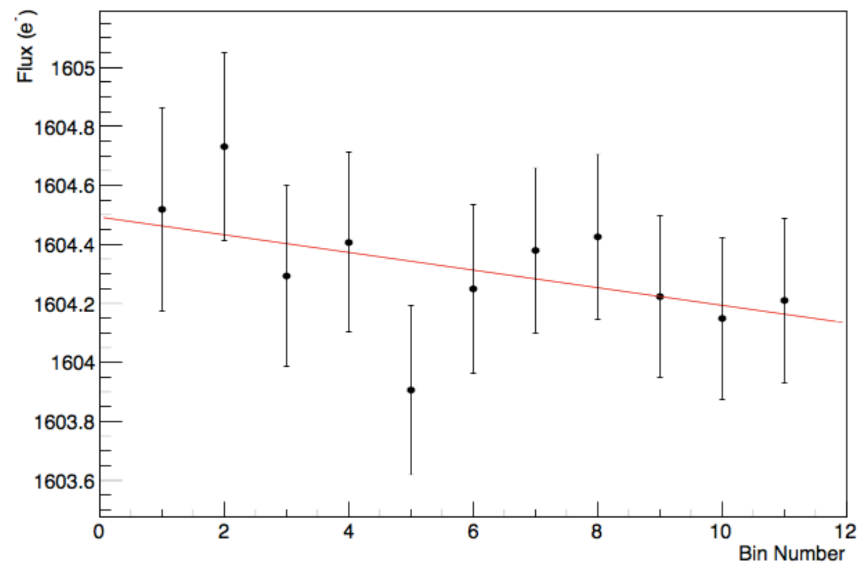

Flux [electrons] along columns

1. Measure slope
2. Apply MC results to convert slope to CTE

LSST spec for parallel CTE: 0.999997

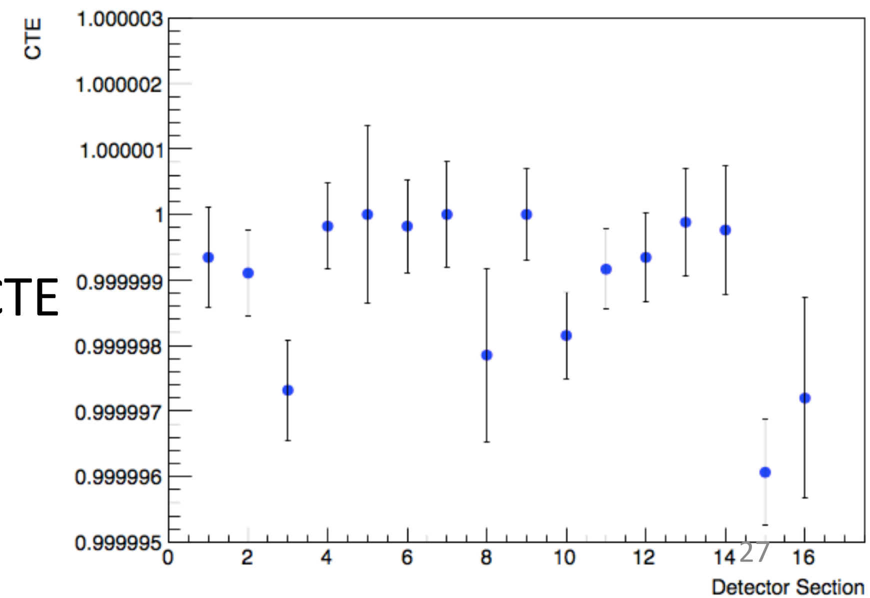

Fe55 hit shape

Edge Effect in Fe55 hit shape

Shear g1 = (a-b)/(a+b)

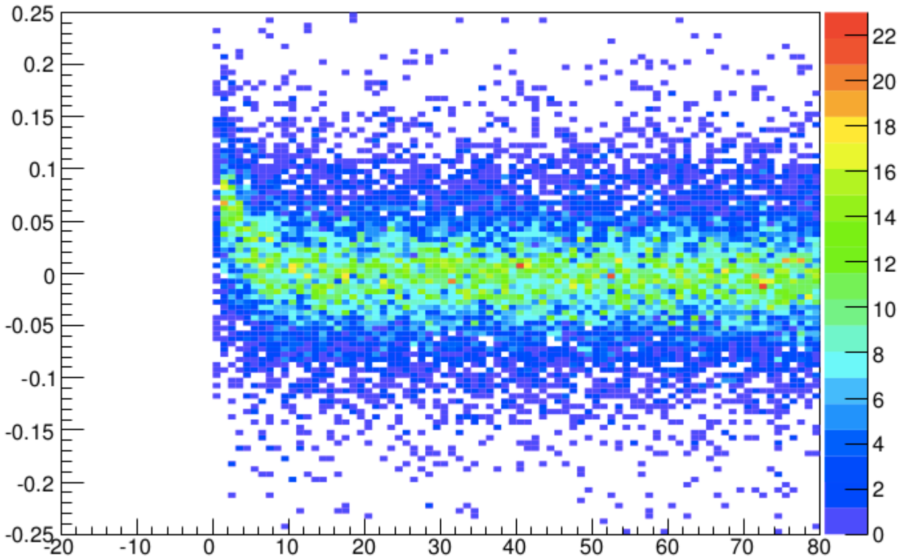

g1 vs X

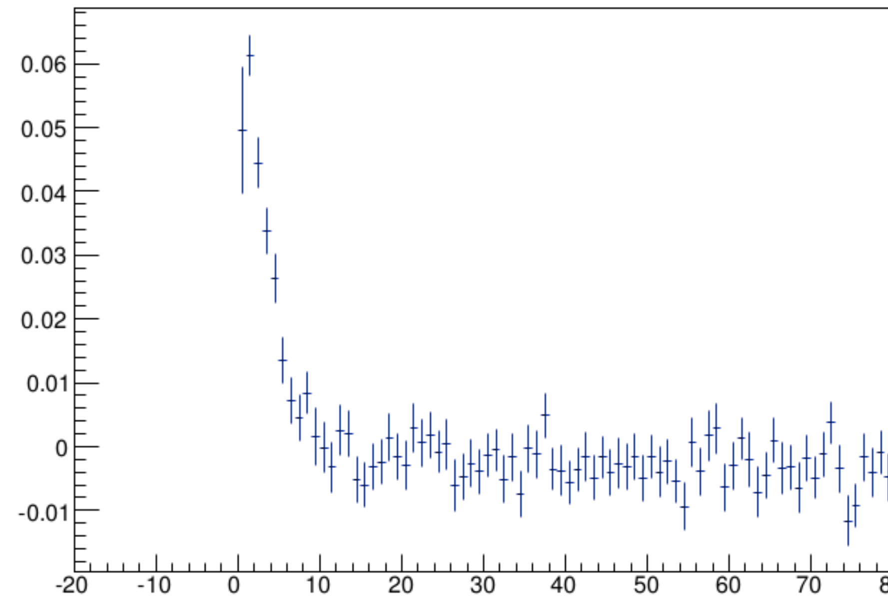

g1 vs X

g1 positive → elongation along x, affects ~ 10 pixels

A. Nomerotski 2015 *JINST* **10** C06010

Sigma (x,y) Map

Center has smaller sigma since average depth of conversion is deeper there, hence less diffusion

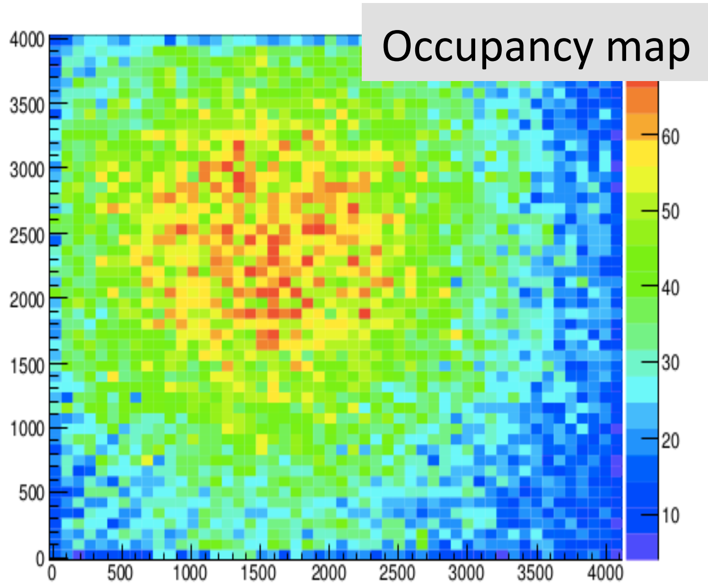

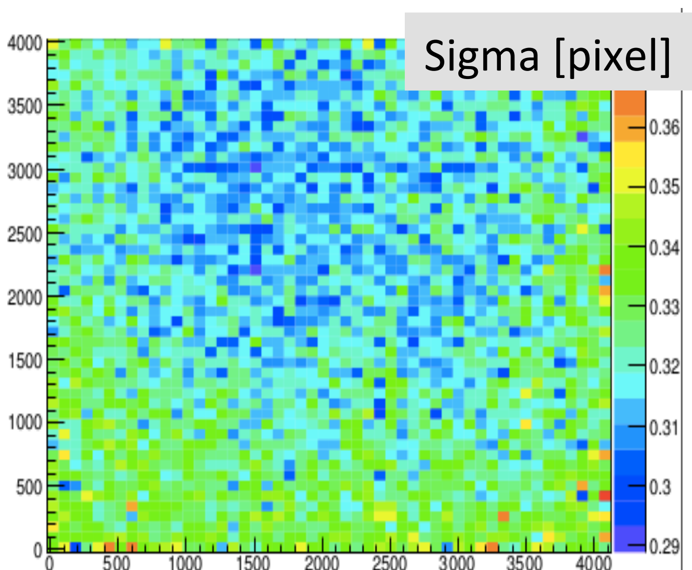

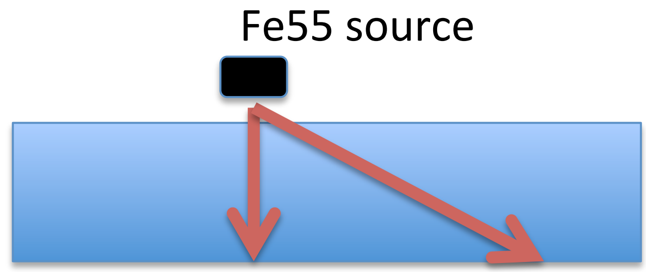

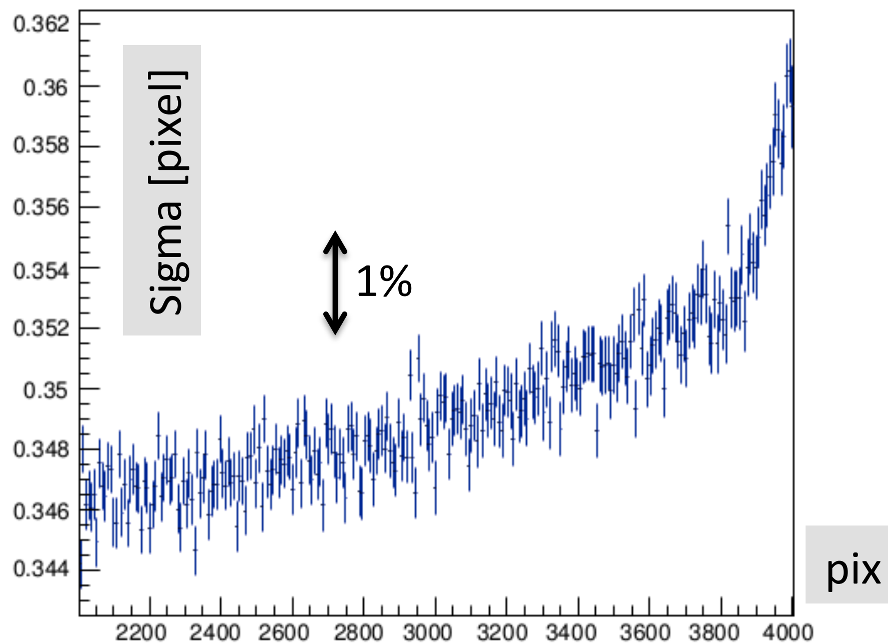

Summary

Thick, fully depleted CCDs have non-trivial electrostatics → leads to distortions of pixel areas, corrections are important for science

LSST has a plan to study and remove these sensor signatures in the data and to model them correctly in science simulations

Fe55 flat fielding is a powerful tool to characterize CCDs

Fe55 can be used to measure CTE even for thick CCDs

Acknowledgements: Paul O'Connor, Ivan Kotov, Peter Takacs, Craig Lage, Andrew Bradshaw, Pierre Astier, Pierre Antilogus, Andy Rasmussen, Dan Weatherill, Merlin Fisher-Levine, Daniel Yates, Jason Brooks, Hyeyun Park, Homer Neal, Woody Gilbertson, Erin Sheldon